Computers & Geosciences 35 (2009) 1247–1254

Contents lists available at ScienceDirect

Computers & Geosciences

journal homepage: www.elsevier.com/locate/cageo

A general-purpose Green's function-based interpolator ☆

Paul Wessel *

Department of Geology and Geophysics, School of Ocean and Earth Science and Technology, University of Hawaii at Manoa, 1680 East-West Road, Honolulu HI 96822, USA

ARTICLE INFO

Article history:
Received 15 April 2008
Received in revised form
17 July 2008
Accepted 1 August 2008

Keywords:
Splines
Green's functions
Interpolation
Gridding

ABSTRACT

A useful approach to data interpolation is to determine the Green's function for the interpolation operator and construct the interpolation from the super-positioning of suitably scaled Green's functions located at the data constraints. Such Green's functions have been determined for Cartesian splines in 1-, 2-, and 3-D, including regularized splines and splines in tension. Furthermore, these techniques have also been extended to spherical surfaces. I present a new command-line tool, greenspline, which acts as a general-purpose interpolator for both Cartesian and spherical surface data. The program runs on all platforms and is compatible with the Generic Mapping Tools.

1. Introduction

Geoscientists are in constant need of resampling raw data at intermediate locations, either for facilitating special processing that requires a constant sampling interval (e.g., spectral analysis) or to prepare graphical representations. Numerous techniques have been developed to accomplish this step, ranging from simple spatial averaging to statistical procedures (e.g., kriging). Perhaps the most common approach involves using splines to fit a surface of minimum curvature to existing data and then evaluate the surface at the desired output locations (e.g., Briggs, 1974; Swain, 1976; Smith and Wessel, 1990). While popular, this method can suffer from erratic oscillations if rapid changes in values or outliers are present in the data. Fortunately, including modest tension in the solution can mitigate many of these artifacts (e.g., Schweikert, 1966). Thus, using continuous curvature splines in tension remains a mainstay of interpolation recipes. Many implementations of these methods rely on complex finite difference (e.g., Swain, 1976; Smith and Wessel, 1990) or finite element techniques (e.g., Renka, 1984; Inoue, 1986). One strength of these implementations is their ability to handle large amounts of data. However, if the data density is very high, almost any gridding method will be relatively successful, and often a simpler approach will yield satisfactory results. When data constraints are more modest (here loosely defined as $n < 10{,}000$) an alternative approach is available, based on the concept of influence or Green's functions (e.g., Courant and Hilbert, 1953; Greenberg, 1971; Roach, 1982; Duffy, 2001; Szmytkowski, 2006, 2007). Here, the Green's function of the gridding operator is determined and the model surface is constructed as a sum of contributions from Green's functions, each weighted by a scale associated with each data constraint (e.g., Sandwell, 1987). Thus, values at any point are obtained by evaluating the Green's function for all distances between the output point and all the input points, each function scaled by a weight, and then summed. There are four distinct benefits to this approach that make it particularly valuable for interpolation: (1) unlike implementations tied to a regular grid, there are no requirements that the input or output locations form any regular lattice—one is at complete freedom to choose the geometry; (2) for interpolation problems where the constraining data are a mix of surface heights and surface slopes, we can easily use the gradient of the Green's

☆ Code available from server at http://www.soest.hawaii.edu/pwessel/pwsoftware

* Tel.: 1 808 956 4778; fax: 1 808 956 5154.
E-mail address: pwessel@hawaii.edu

0098-3004/$ - see front matter © 2008 Elsevier Ltd. All rights reserved.
doi:10.1016/j.cageo.2008.08.012

function to include the slope constraints; (3) if derivatives of the solution are desired then these can be accurately evaluated analytically from the Green's function, thus avoiding approximations by finite-difference operations on the surface grid; and (4) the implementation of the solution is extremely simple, lending itself to rapid deployment in custom environments without significant resources being allocated to the development. Here, I give a brief overview of the method and present an implementation in the POSIX C language. Eventually, the program will be included in the Generic Mapping Tools (Wessel and Smith, 1998).

2. Interpolation with Green's functions for splines

In this Section I will outline some of the basic equations used for spline interpolation using Green's functions; consult the literature for more details (Sandwell, 1987; Mitás and Mitásova, 1988; Mitásová and Hofierka, 1993; Mitásová and Mitás, 1993; Wessel and Bercovici, 1998; Wessel and Becker, 2008). Solutions by Green's functions imply that the surface $w(\mathbf{x})$ can be expressed as

$$w(\mathbf{x}) = T(\mathbf{x}) + \sum_{j=1}^{n} \alpha_j g(\mathbf{x}, \mathbf{x}_j), \tag{1}$$

where $\mathbf{x}$ is the output location, g is the Green's function, $\mathbf{x}_j$ is the location of the jth data constraint, and α_j are the associated unknown weights. Here, $T(\mathbf{x})$ is a trend function that captures variations that may not be possible to express via the Green's functions (typically a constant) or a regional trend that we first remove from the data constraints. The weights α_j are determined by requiring Eq. (1) to be satisfied exactly at the n data locations, i.e.

$$w(\mathbf{x}_i) = \sum_{j=1}^{n} \alpha_j g(\mathbf{x}_i, \mathbf{x}_j), \quad i = 1,\ n, \tag{2}$$

yielding a n by n square linear system which is solved for α_j. Should there be m surface slope constraints s_k in the directions $\mathbf{n}_k$ among the n overall constraints then the m linear equations for these constraints may be included in the linear system as the additional equations

$$s(\mathbf{x}_k) = \nabla w(\mathbf{x}_k)\mathbf{n}_k = \sum_{j=1}^{n} \alpha_j \nabla g(\mathbf{x}_k, \mathbf{x}_j)\mathbf{n}_k, \quad k = 1,\ m. \tag{3}$$

Slope constraints are most helpful for phenomena that are well behaved and have continuous and smoothly varying gradients. The Green's function itself must satisfy the inhomogeneous partial differential equation

$$\nabla^2[\nabla^2 - p^2]g(\mathbf{x}, \mathbf{x}') = \delta(\mathbf{x} - \mathbf{x}'), \tag{4}$$

where ∇^2 is the Laplacian operator, δ is the Dirac Delta function, and p is the tension (which may be 0 for a minimum curvature solution). Solving Eq. (4) requires us to express ∇^2 and δ in the pertinent coordinates system (Cartesian or spherical), resulting in different Green's functions $g(\mathbf{x}, \mathbf{x}')$. It is also possible to require that derivatives higher than the curvature should exist and be continuous as well, leading to generalized splines in tension (e.g., Mitásová and Mitás, 1993). Table 1 summarizes the Green's functions for splines in tension (or no tension) that have been used for interpolation in the literature; Fig. 1 shows all the isotropic functions and their gradients for some values of the tension parameters. Note

Table 1
Ten Green's functions and their gradients for published splines.

		g	$\lvert\nabla g\rvert$	Ref.
Cartesian 1-D:				
1	$p=0$	r^3	r	1
2	$p>0$	$e^{-pr}+pr-1$	$1-e^{-pr}$	2
Cartesian 2-D:				
3	$p=0$	$r^2(\ln r-1)$	$r(2\ln r-1)$	1
4	$p>0$	$K_0(pr)+\log(pr)$	$(1/pr)-K_1(pr)$	2,3
5[a]	$p>0$	$-\ln\lvert(pr/2)^2\rvert-E_1\lvert(pr/2)^2\rvert-\gamma$	$-2((1-\exp[(pr/2)^2])/r)$	3
Cartesian 3-D:				
6	$p=0$	r	1	1
7	$p>0$	$(1/pr)(e^{-pr}-1)+1$	$(1/pr^2)[1-e^{-pr}(pr+1)]$	2
8	$p>0$	$\frac{1}{pr}\mathrm{erf}\left(\frac{pr}{2}\right)-\frac{1}{\sqrt{\pi}}$	$\frac{\frac{pr}{\sqrt{\pi}}e^{-(pr/2)^2}-\mathrm{erf}\left(\frac{pr}{2}\right)}{pr^2}$	3
Spherical surface:				
9	$p=0$	$\mathrm{dilog}(\sin^2\theta/2)$	$\log(\sin\theta/2)\cot\theta/2$	4,5
10[b]	$p>0$	$(\pi P_\nu(-\cos\theta)/\sin\nu\pi)-\log(1-\cos\theta)$	$(\pi(\nu+1)/\sin\nu\pi\sin\theta)[\cos\theta P_\nu(-\cos\theta)+P_{\nu+1}(-\cos\theta)]+\cot\theta/2$	5

Notes: $r=\lvert\mathbf{x}-\mathbf{x}'\rvert$, $\theta=\cos^{-1}(\mathbf{x}\cdot\mathbf{x}')$, K_j is modified Bessel function of second kind of order j, E_1 is exponential integral, erf is error function, dilog is Euler's dilogarithm, and P_ν is associated Legendre function of first kind.

Refs.: 1 = Sandwell (1987), 2 = Wessel and Bercovici (1998), 3 = Mitásová and Mitás (1993), 4 = Parker (1994), 5 = Wessel and Becker (2008).

[a] Euler's constant $\gamma = 0.577215\ldots$

[b] $p^2 = -\nu(\nu+1)$.

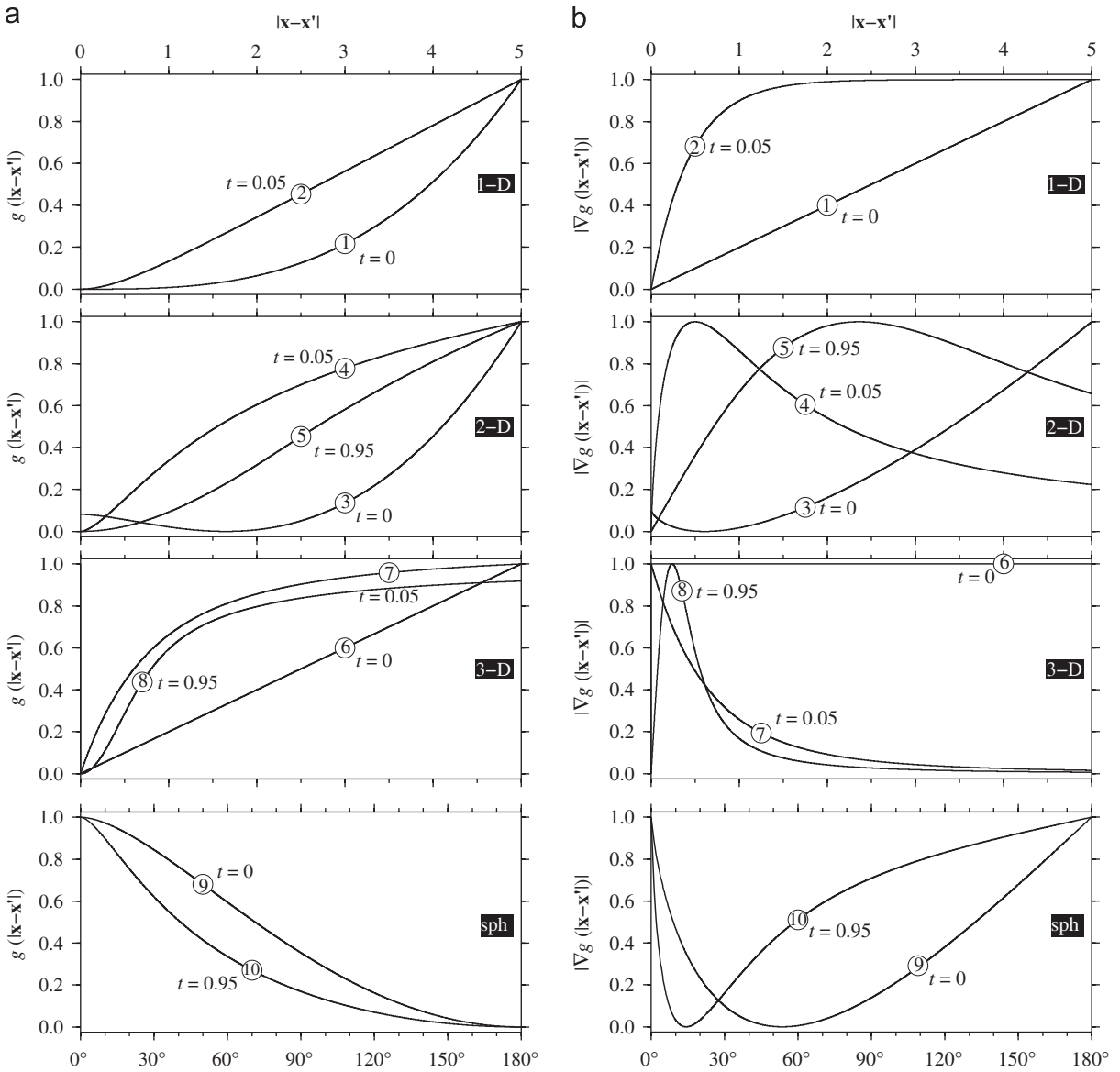

Fig. 1. (a) Typical shapes of 10 Green's functions discussed in text, arranged by spatial geometry. All curves have been normalized for chosen domain. Arbitrary values were chosen for those functions that use tension. Curves, for each dimension, differ in how they distribute weights to proximal and distal data constraints. (b) Gradients of 10 Green's functions. As derivatives amplify short-wavelength information, gradients give higher weight to values near node. Circled numbers refer to Green's functions listed in Table 1.

we will typically specify the tension p via the auxiliary variable t. The two parameters are related via $p^2 = t/(1-t)$ which conveniently compresses the full range of tensions into the normalized range $0 \leqslant t < 1$.

3. Implementation

I have implemented the interpolation solution (1) in the program greenspline.c which can handle various input data scenarios (e.g., mixed tables of height and slope constraints), different geometries (Cartesian 1-, 2-, and 3-D, as well as spherical surface), tension or no tension, and output scenarios (regular lattice, arbitrary output locations) of the resulting surface or its directional derivative. The bulk of the program concerns itself with building the n by n square matrix equation, solving for the weights α_j, and evaluating the solution at the output locations. The default approach is to solve the matrix equation using a standard Gauss–Jordan solver. Despite using double precision, the inversion can become numerically unstable if some data points are very closely spaced relative to the overall span of the data. This problem can be partly overcome by preprocessing the data (e.g., by averaging closely spaced neighbors). Alternatively, one can choose to solve the linear system using singular value

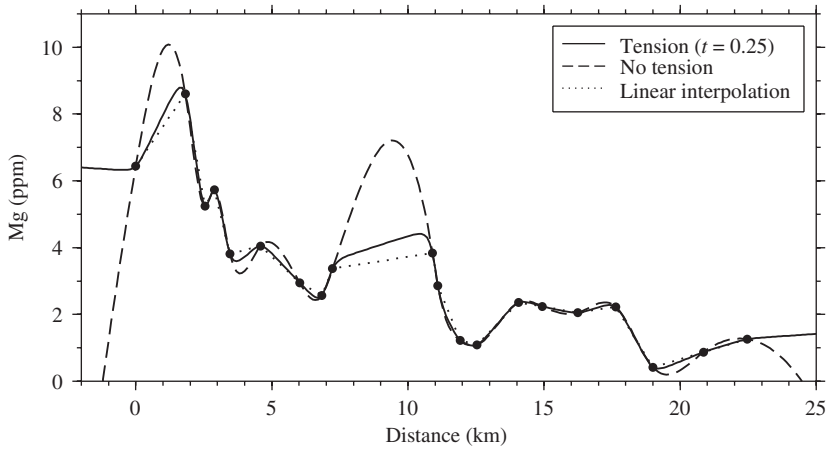

Fig. 2. Example of 1-D splines, here interpolating a data set of magnesium concentrations given as a function of distance upstream from a river mouth, taken from Davis (1986). A spline in tension is a good compromise between linear limit of a piecewise linear interpolant and smooth but exaggerated oscillations of a cubic spline.

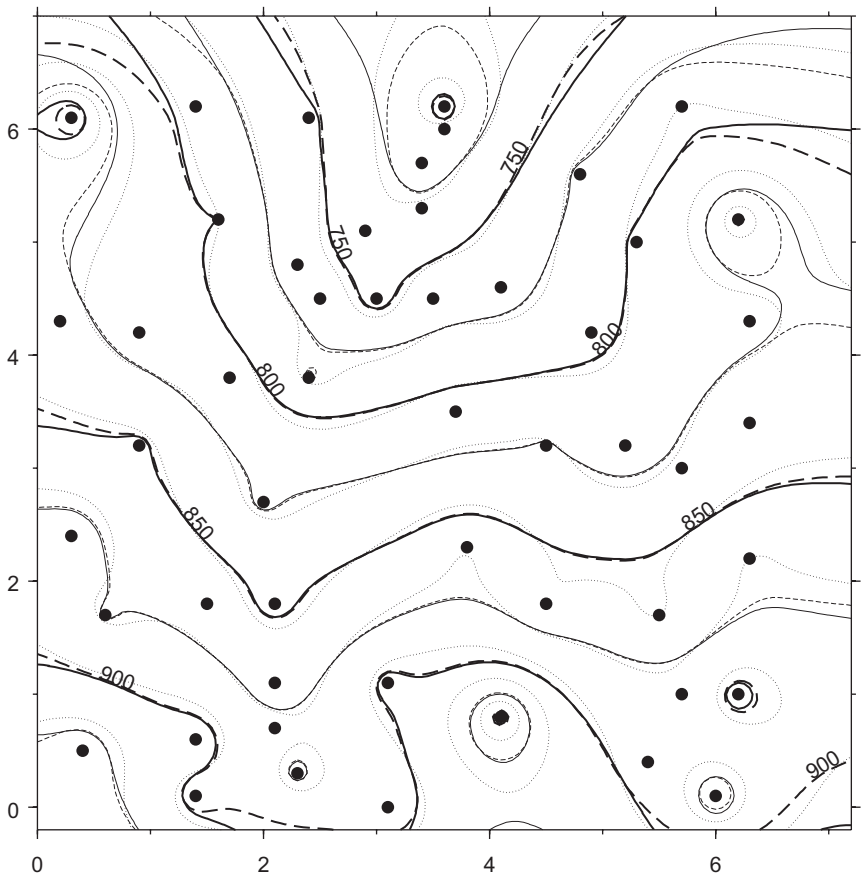

Fig. 3. Three examples of 2-D Cartesian interpolation using a topographic data set (solid circles) from Davis (1986). Solid contours represent spline-in-tension ($t = 0.5$) interpolation, dashed lines same tension but using GMT's finite difference implementation (Smith and Wessel, 1990), and finally regularized spline in tension (Mitásová and Mitás, 1993) using $t = 0.99$ (dotted contours).

decomposition and ignore the contributions associated with the smallest eigenvalues. This approach gives a smoother solution that no longer interpolates the data exactly.

The program is written as a supplement to the Generic Mapping Tools (Wessel and Smith, 1998) and requires GMT for its installation. The supplement will most likely

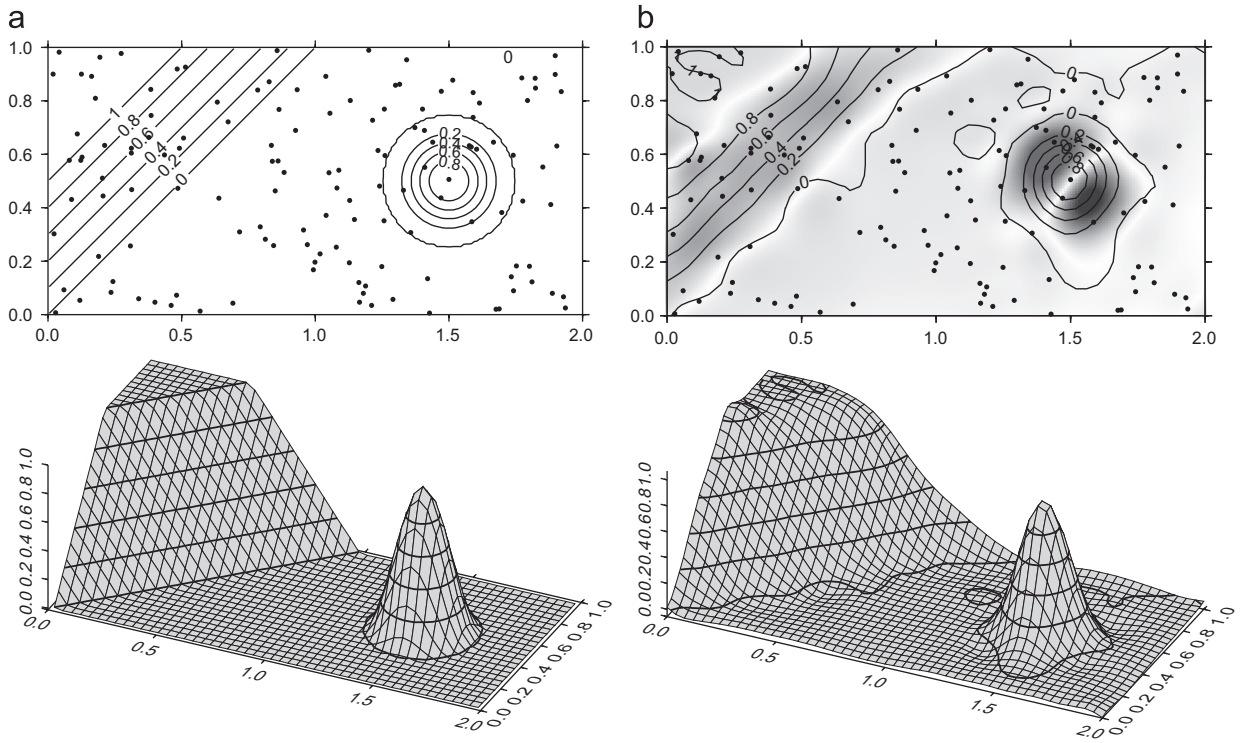

Fig. 4. (a) Synthetic data set containing two flat regions separated by a linear slope, with a Gaussian peak placed on lower level (Lancaster and Salkauskas, 1980). This function was then randomly sampled at 150 locations (solid circles on contour map). (b) Interpolation of 150 irregularly spaced data samples using regularized spline in tension ($t = 0.998$). For upper panel we also evaluated analytically gradient of solution in N135°E direction and display it in shades of gray.

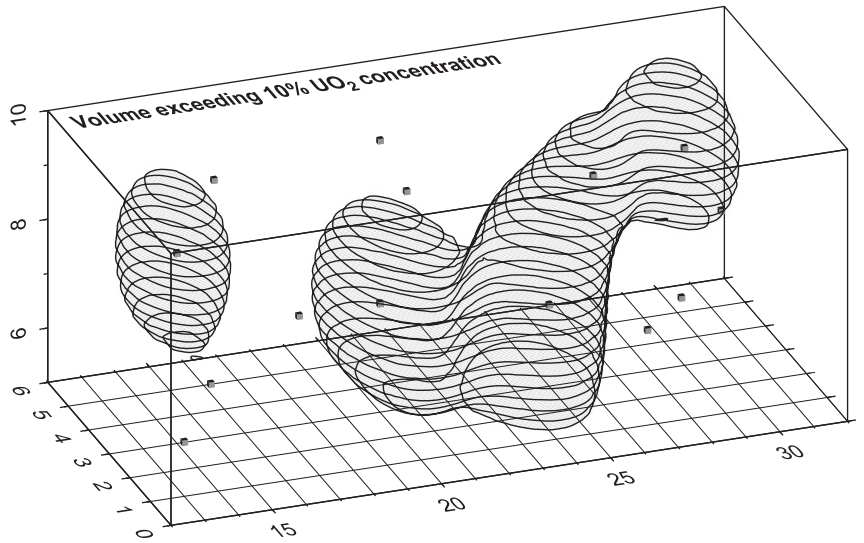

Fig. 5. 3-D estimates of uranium oxide concentrations in a carnotite body in Jurassic sediments in Colorado Plateau (Davis, 1986). Data points (shaded cubes) were gridded using regularized spline in tension in 3-D ($t = 0.85$) and contoured every 0.25 feet in elevation. We see two separate volumes having concentrations in excess of 10%.

be included into the main GMT suite at the next release point. Implemented in the highly portable C POSIX language, greenspline may be run under any operating system. In addition to source code, documentation, data and command lines for all the examples shown herein, and executables for several architectures (Windows, OS X, Linux, and Solaris) are available from the author's website (www.soest.hawaii.edu/pwessel/greenspline).

4. Examples

Here I will briefly demonstrate usage of greenspline for each spatial dimension for various splines. Examples (including command lines and test data sets) for all possible uses of greenspline are distributed with the program and can be used to determine how to invoke greenspline for particular scenarios. I will examine the results of some of these examples.

4.1. 1-D interpolation

Simple 1-D interpolation is typically done with some variation of cubic splines where cubic segments are linked by requiring continuity of value and its first two derivatives. Here, greenspline will instead compose a global solution (as opposite of piecewise) from a sum of suitably scaled Green's functions. I have chosen a data set from Davis (1986) who presented magnesium

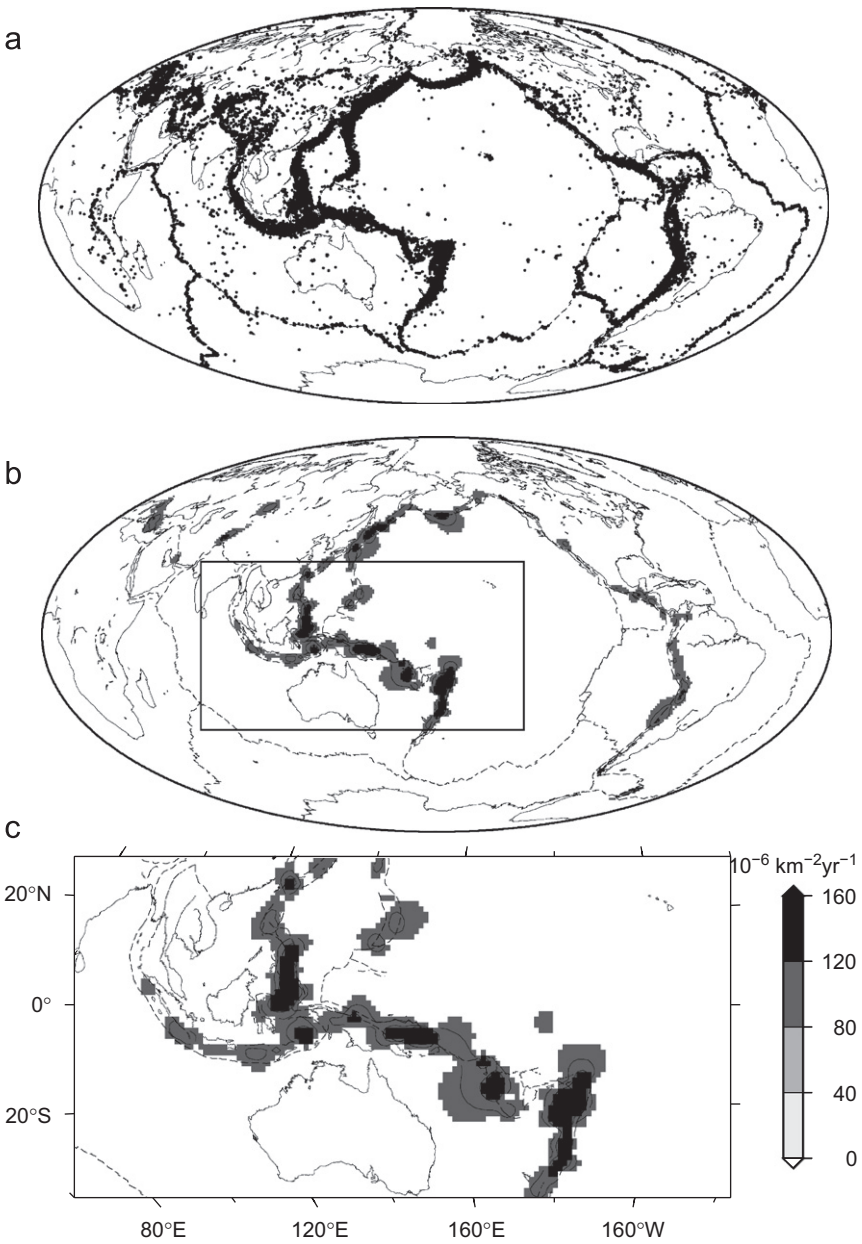

Fig. 6. (a) Distribution of earthquakes since 1957 with magnitude >5. (b) Shaded level global map of average number of earthquakes per km^2 per year (times 10^6) obtained using a spherical surface spline in tension ($t = 0.9999$). (c) Details of global solution for northern plate boundary of Australia. Plate boundaries are drawn as dashed lines.

concentrations (in ppm) detected as a function of distance upstream from a river mouth. Interpolations were done with both the minimum curvature spline of Sandwell (1987) as well as the spline in moderate tension of Wessel and Bercovici (1998). Both solutions and the data constraints are shown in Fig. 2; the dotted line is the linear interpolant shown as a reference curve. We note that cubic splines tend to overshoot dramatically in unconstrained areas where there are rapid changes in the gradient; tension can mitigate these limitations, with a linear spline as its end member case (dotted line in Fig. 2). Boundary conditions on the slopes can also be specified as gradient constraints. Although not shown here, parametric curves in higher dimensions can be determined by interpolating each spatial coordinate as a function of the common parameter (typically time or distance along the path).

4.2. 2-D interpolation

With Cartesian data we may choose among three different spline functions. The first two are the 2-D equivalents of the splines encountered in the previous section. We will demonstrate the difference between the spline in tension implemented here versus the finite-difference implementation used by the GMT tool surface (Smith and Wessel, 1990). When the same data set is used as data constraints we note the two solutions differ most significantly close to the edges of the region (Fig. 3). The reason for these discrepancies has to do with the boundary conditions. In greenspline we utilize free-space Green's functions so there is no boundary condition applied at the domain boundaries. In contrast, GMT's surface applies specific boundary conditions such as zero curvature along the edges. For most interpolation tasks this difference is arbitrary and inconsequential, but if the data interpolated reflect a phenomenon known to obey certain conditions then a finite-difference implementation can better satisfy such constraints. However, note that Eq. (3) can be used to satisfy surface gradient conditions along the boundary or even internally. For further comparison we also show the regularized spline in tension (dotted contours). While following the other two solutions, the generalized solution tend to be somewhat smoother near data constraints as it retains higher derivatives; however, due to differences in the Green's functions the two tension values ($t = 0.5$ and $t = 0.99$) do not directly compare.

In Fig. 4a we show the synthetic data set of Lancaster and Salkauskas (1980) (their Fig. 7.13). As in their example, this model was sampled at 150 random locations (dots in contour map) and used as data constraints for the 2-D interpolation problem. Fig. 4b shows the surface that was obtained using a regularized spline in tension ($t = 0.998$). A reasonably good fit is obtained given the data distribution. The contour map also shows the gradient of the solution in the N135°E direction that was obtained analytically from Eq. (1).

4.3. 3-D interpolation

Our final Cartesian example involves a data set of 36 uranium oxide concentrations obtained from Jurassic sandstone on the Colorado Plateau (Davis, 1986). We chose to grid these using the 3-D regularized spline in tension operator ($t = 0.85$) and display the outline of the volume in which the UO_2 concentration exceeds 10% (Fig. 5). As is typical of the regularized spline (Mitásová and Hofierka, 1993) we had to try a range of tension values to find a range for which the solutions were stable.

4.4. 2-D spherical interpolation

Our last example pertains to interpolation on a spherical surface. We have taken the global catalog of earthquakes since 1957 whose magnitude exceeded 5.0 (Fig. 6a) and determined the number of earthquakes per km^2 averaged over $3^\circ \times 3^\circ$ blocks (not all blocks had earthquakes). These densities were then interpolated onto a global $1^\circ \times 1^\circ$ grid using the spherical surface spline in tension of Wessel and Becker (2008), and values below a threshold were set to NaN (IEEE not-a-number) in order to suppress any negative oscillations that even the high tension ($t = 0.9999$) did not fully suppress. The resulting grid was gray shaded and contoured every 20 units (Fig. 6b). Finally, we zoom in on the northern plate boundary of Australia to see more details (Fig. 6c).

Acknowledgments

This work was supported by Grant OCE-0452126 from the US National Science Foundation and It is SOEST contribution no. 7616. Helpful reviews by David Sandwell and Neil Mitchell improved the manuscript.

References

Briggs, I.C., 1974. Machine contouring using minimum curvature. Geophysics 39 (1), 39–48.
Courant, R., Hilbert, D., 1953. Methods of Mathematical Physics, Vol. 1. Interscience, New York pp 560.
Davis, J.C., 1986. Statistics and Data Analysis in Geology. Wiley, New York pp 646.
Duffy, D.G., 2001. Green's Functions with Applications. Chapman and Hall/CRC, Boca Raton, FL pp 443.
Greenberg, M.D., 1971. Application of Green's Functions in Science and Engineering. Prentice-Hall, Englewood Cliffs, NJ pp 141.
Inoue, H., 1986. A least-squares smooth fitting for irregularly spaced data: finite-element approach using the cubic B-spline basis. Geophysics 51 (11), 2051–2066.
Lancaster, P., Salkauskas, K., 1980. Curve and Surface Fitting: An Introduction. Academic Press, London, UK pp 280.
Mitás, L., Mitásova, H., 1988. General variational approach to the interpolation problem. Computers and Mathematics with Applications 16 (12), 983–992.
Mitásová, H., Hofierka, J., 1993. Interpolation by regularized spline with tension: II. Application to terrain modeling and surface geometry analysis. Mathematical Geology 25 (6), 657–669.
Mitásová, H., Mitás, L., 1993. Interpolation by regularized spline with tension: I. Theory and implementation. Mathematical Geology 25 (6), 641–655.
Parker, R.L., 1994. Geophysical Inverse Theory. Princeton University Press, Princeton, NJ pp 386.
Renka, R.J., 1984. Interpolation on the surface of a sphere. ACM Transaction of Mathematical Software 10 (4), 437–439.
Roach, G.F., 1982. Green's Functions. Cambridge University Press, Cambridge, UK pp 344.
Sandwell, D.T., 1987. Biharmonic spline interpolation of Geos-3 and Seasat altimeter data. Geophysical Research Letters 14 (2), 139–142.
Schweikert, D.G., 1966. An interpolating curve using a spline in tension. Journal of Mathematical Physics 45 (3), 312–317.

Smith, W.H.F., Wessel, P., 1990. Gridding with continuous curvature splines in tension. Geophysics 55 (3), 293–305.
Swain, C.J., 1976. A FORTRAN IV program for interpolating irregularly spaced data using the difference equations for minimum curvature. Computers & Geosciences 1 (4), 231–240.
Szmytkowski, R., 2006. Closed form of the generalized Green's function for the Helmholtz operator on the two-dimensional unit sphere. Journal of Mathematical Physics 47 (063506), 1–11.
Szmytkowski, R., 2007. Closed forms of the Green's function and the generalized Green's function for the Helmholtz operator on the N-dimensional unit sphere. Journal of Physics A: Mathematical and Theoretical 40, 995–1009.
Wessel, P., Becker, J.M., 2008. Interpolation using a generalized Green's function for a spherical surface spline in tension. Geophysical Journal International 174, 21–28.
Wessel, P., Bercovici, D., 1998. Interpolation with splines in tension: a Green's function approach. Mathematical Geology 30 (1), 77–93.
Wessel, P., Smith, W.H.F., 1998. New, improved version of Generic Mapping Tools released. Eos Transactions, AGU (American Geophysical Union) 79 (47), 579.